Coherent Manipulation and Decoherence of S=10 Single-Molecule Magnets

Susumu Takahashi,[1, *] Johan van Tol,[2] Christopher C. Beedle,[3] David
N. Hendrickson,[3] Louis-Claude Brunel,[2, †] and Mark S. Sherwin[1]

[1]*Department of Physics and Center for Terahertz Science and Technology,
University of California, Santa Barbara, California 93106*
[2]*National High Magnetic Field Laboratory, Florida State University, Tallahassee Florida 32310*
[3]*Department of Chemistry and Biochemistry, University of California, San Diego, La Jolla, California 92093*
(Dated: November 5, 2008)

We report coherent manipulation of S=10 Fe$_8$ single-molecule magnets. The temperature dependence of the spin decoherence time T_2 measured by high frequency pulsed electron paramagnetic resonance indicates that strong spin decoherence is dominated by Fe$_8$ spin bath fluctuations. By polarizing the spin bath in Fe$_8$ single-molecule magnets at magnetic field $B = 4.6$ T and temperature $T = 1.3$ K, spin decoherence is significantly suppressed and extends the spin decoherence time T_2 to as long as 712 ns. A second decoherence source is likely due to fluctuations of the nuclear spin bath. This hints that the spin decoherence time can be further extended via isotopic substitution to smaller magnetic moments.

PACS numbers: 76.30.-v, 75.50.Xx, 03.65.Yz

Single-molecule magnets (SMMs) behave like nanoscale classical magnets at high temperatures [1]. The quantum mechanical nature of SMMs emerges at low temperatures with behaviors like quantum tunnelling of magnetization (QTM) [2, 3, 4], quantum phase interference of two tunnelling paths [5, 6] and the observation of discrete transitions in electron paramagnetic resonance (EPR) and optical spectroscopy [1, 7, 8, 9, 10]. As quantum magnets based on solid state systems, SMMs form a unique class of materials that have a high-spin, and their spin state and interaction can be easily tuned by changing peripheral organic ligands and solvate molecules. Because the molecules within the crystal lattice of SMMs interact very weakly with each other, properties of a single SMM can be deduced from measurements of a macroscopic ensemble.

Although quantum phenomena observed in SMMs have been investigated extensively, couplings between SMMs and their environment are still poorly understood. Coupling to the environment results in decoherence, which must be understood to optimize SMMs for proposed applications to dense and efficient quantum memory, computing, and molecular spintronics devices [11, 12]. With pulsed EPR, it is possible to directly measure spin relaxation times. However measurement of pulsed EPR for high-spin SMMs has been extremely challenging due to strong spin decoherence [13]. To our knowledge, no direct measurements of the spin relaxation times have been reported for single crystals of SMMs. Various investigations of spin dynamics have led to the *estimate* that the lower bound of spin decoherence time (T_2) in high-spin SMMs is on the order of nanosec-

onds [9, 13, 14]. Decoherence of SMMs must therefore be suppressed in order to measure T_2. One approach to reduce spin decoherence has been to reduce the number of spins in the bath. Molecule-based magnets have been studied employing highly dilute solutions. Thereby, minimizing intermolecular interactions leads to an increase of T_2 [15, 16]. However, these compounds may have different quantum and magnetic properties from those of single crystals. Another approach has been to reduce the fluctuations within spin baths. When the spin bath is fully polarized, the spin bath fluctuations are completely eliminated. For dilute, isotropic spins on nitrogen-vacancy (NV) centers in diamond, spin decoherence due to electron spins has been quenched by complete polarization (> 99%) of the electron spin baths with application of high magnetic fields and low temperatures [17].

This paper presents measurements of the spin decoherence time T_2 of single crystals of the $S = 10$ SMM [Fe$_8$(O)$_2$(OH)$_{12}$(C$_6$H$_{15}$N$_3$)$_6$]Br$_7$(H$_2$O)Br·8H$_2$O, abbreviated Fe$_8$ [18]. pulsed EPR spectroscopy at 240 GHz and 4.6 T is used to measure T_2. The energy difference between $m_S = -10$ and $m_S = -9$ states is 11.5 K, so Fe$_8$ SMMs are almost completely polarized to the $m_S = -10$ lowest lying state below 1.3 K. At 1.3 K, T_2 was measured to be 712 ns. Upon raising the temperature to 2 K, the T_2 decreased by nearly 1 order of magnitude. As temperature increases, so do fluctuations of the SMM spin bath. In order to describe the temperature dependence, we extend a model of spin decoherence time for a $S = 1/2$ system to a system with arbitrary S. Good agreement between the data and the model for Fe$_8$ SMMs strongly supports the spin decoherence caused by fluctuations of Fe$_8$ SMMs spin bath. We also show that there exist other decoherence sources likely caused by proton and ^{57}Fe nuclear magnetic moments which limit the spin decoherence time $T_2 \sim 1$ μs.

The magnetic properties of the $S = 10$ Fe$_8$ SMM are
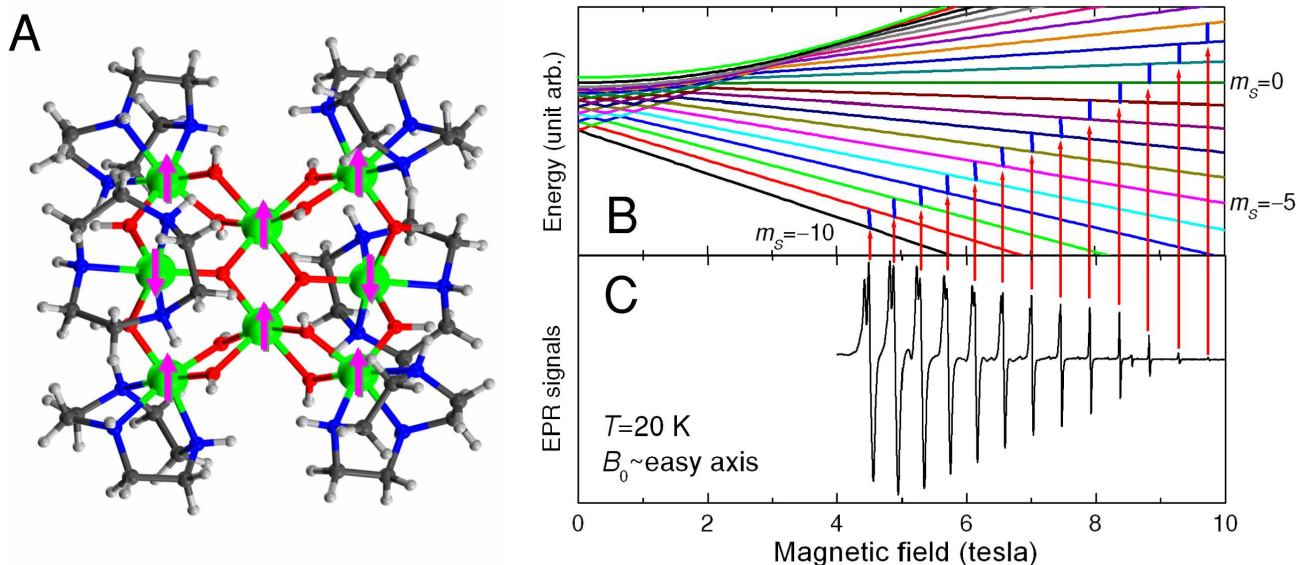
FIG. 1: (A) Schematic diagram of Fe$_8$ molecule (Fe: Green, O: Red, N: Blue, C: Gray and H: White). The Fe$_8$ molecule consists of eight Fe(III) ($S = 5/2$) ions which couple to each other to form an $S = 10$ ground state. (B) Energy diagram as a function of the magnetic field, $\boldsymbol{B}_0$ while the magnetic field is applied along the easy axis. The diagram is calculated using Equation (1). (C) cw EPR spectrum at 20 K taken by sweeping magnetic fields from 4 T to 10 T. The magnetic field is applied along the easy-axis within 10 degrees. Corresponding EPR transitions are indicated by blue solid lines in Fig. 1(B). The spectrum also shows fine structures which are more pronounced in the transitions of high $|m_S|$ values. These were also seen in previous studies [1]. A resonance at 8.5 T is a spurious signal from impurities in the sample holder.

well-described by the following spin Hamiltonian,

$$H = \mu_B g \boldsymbol{S} \cdot \boldsymbol{B}_0 + D S_z^2 + E(S_x^2 - S_y^2), \qquad (1)$$

where μ_B is the Bohr magneton, $\boldsymbol{B}_0$ is the magnetic field and S are the spin operators. The parameter $g = 2.00$ is an isotropic g-factor and $D = -6.15$ GHz and $E = 1.14$ GHz represent the second order anisotropy constants [1]. The large spin ($S = 10$) and the negative D value lead to a large energy barrier between the spin-up and spin-down states. Higher order terms are not included here. As shown in the energy diagram as a function of the magnetic field given in Fig. 1(B), at low magnetic fields there are many energy level anti-crossings which are the origin of quantum tunneling of magnetization [1, 2, 3]. On the other hand, in a high magnetic field regime, where the magnetic field is aligned along the easy axis and is higher than 4.3 T, there are no level anti-crossings (see Fig. 1(B)).

Experiments were performed with the 240 GHz cw and pulsed EPR spectrometer at the National High Magnetic Field Laboratory (NHMFL), Tallahassee FL, USA. For this study, we employed a superheterodyne quasioptical bridge with a 40 mW solid-state source. In order to enable *in situ* rotation of the sample relative to the applied magnetic field, we employed a rotating sample holder mounted with its axis perpendicular to a 12.5 T superconducting solenoid. A detailed description of the

setup is given elsewhere [19, 20]. Measurements were performed on Fe$_8$ single crystal samples whose magnetic anisotropic axis, called the easy axis, was identified by X-ray diffraction measurements. Fig. 1(C) shows the cw EPR spectrum at 20 K while the magnetic field was applied along the easy axis within 10 degrees. The applied microwave and field modulation intensities were carefully tuned so as not to distort the EPR lineshape. As indicated in Fig. 1(B) and (C), the spectrum shows EPR transitions ranging from $m_S = -10 \leftrightarrow -9$ at 4.6 T to $m_S = 2 \leftrightarrow 3$ at 9.7 T. In addition, much weaker EPR signals from the $S = 9$ excited state transitions were observed [21].

The temperature dependence of the spin decoherence time (T_2) has been investigated using pulsed EPR at 240 GHz. The spin decoherence time was measured by a Hahn echo sequence ($\pi/2 - \tau - \pi - \tau - echo$) where the delay τ is varied [22]. The width of the pulses was adjusted to maximize the echo signals and was typically between 200 ns and 300 ns. Because the corresponding excitation bandwidth of the applied pulses ($\sim$0.15 mT width) was much smaller than the EPR linewidth, a very small portion of Fe$_8$ spins was actually manipulated in the T_2 measurement. Fig. 2(A) shows echo signals with different delays and the echo area as a function of the delay for the transition of $m_S = -10 \leftrightarrow -9$ at $T = 1.27 \pm 0.05$ K. The spin decoherence time T_2 is estimated from

the decay rate of the echo area which is well fit by a single exponential function, $exp(-2\tau/T_2)$ (Fig. 2(A)). The inset of Fig. 2(A) shows the result of echo-detected field-sweep EPR at $T = 1.27 \pm 0.05$ K which shows the EPR transitions from $m_S = -10 \leftrightarrow -9$. Like cw EPR, the echo-detected EPR shows fine structures. Although the magnetic field was swept up to 12 T, no echo-detected EPR signals corresponding to other transitions were observed. T_2 was measured between $T = 1.93 \pm 0.05$ K and 1.27 ± 0.05 K while a 4.566 T magnetic field was applied along the easy axis. Above 1.93 K, T_2 became too short to give spin echoes within the limited time resolution of the pulsed spectrometer. Within this temperature range, the T_2 shows a strong temperature dependence and increases from $T_2 = 93 \pm 6$ ns at 1.93 ± 0.05 K to $T_2 = 714 \pm 15$ ns at 1.27 ± 0.05 K (see inset of Fig. 3). In addition, we measured the temperature dependence of T_2 with the field orientation along the hard plane which shows a similar temperature dependence (not shown).

The spin-lattice relaxation time T_1 was also investigated at $T = 1.27 \pm 0.05$ K using a stimulated echo sequence ($\pi/2 - \tau - \pi/2 - T - \pi/2 - \tau - echo$) where the delay T is varied [22]. As shown in Fig. 2(B), we found two relaxation rates in the echo decay curve with a short time of $T_{short} = 1.0 \pm 0.1$ μs and a long time of $T_{long} = 948 \pm 108$ μs which both are longer than T_2. Because of the small excitation bandwidth, a strong spectral diffusion is expected. Therefore we currently speculate that the T_{short} is due to spectral diffusion and the T_{long} is the spin-lattice relaxation time T_1. However this value of T_1 is more than two orders of magnitude longer than previous findings [23, 24]. A more detailed investigation of the T_1 processes will be presented elsewhere.

Observation of a strong temperature dependence of T_2 suggests that the main decoherence mechanism at higher temperatures is due to dipolar coupling to fluctuating neighboring electron spins which is often pictured as an electron spin bath [17, 25]. Since the cw EPR spectra show that Fe_8 SMMs dominate the population of electron spins in the sample crystal, the source of the Fe_8 spin decoherence is fluctuations of the Fe_8 spin bath itself which is formed by intermolecularly dipolar-coupled Fe_8 SMMs. At $B_0 = 4.6$ T, where the magnetic field is above all anti-level crossings and single spin flips are suppressed, the Fe_8 spin bath fluctuation is dominated by an energy-conserving spin flip-flop process. This spin flip-flop rate is proportional to the number of pairs of m_S and $m_S \pm 1$ spins and therefore it strongly depends on the spin bath polarization [17, 26]. At 1.27 K and 4.6 T, 99 % of the Fe_8 spin bath is polarized to the $m_S = -10$ lowest lying state which reduces the spin flip-flop rate significantly. Thus, this experiment tests if the main decoherence mechanism of the Fe_8 SMM is the Fe_8 spin bath fluctuation. To test the hypothesis of spin bath decoherence by other SMMs, we extend the case of the two-level system [17, 26] to a multi-level system. Here we obtain the relationship between T_2 and the spin flip-flop
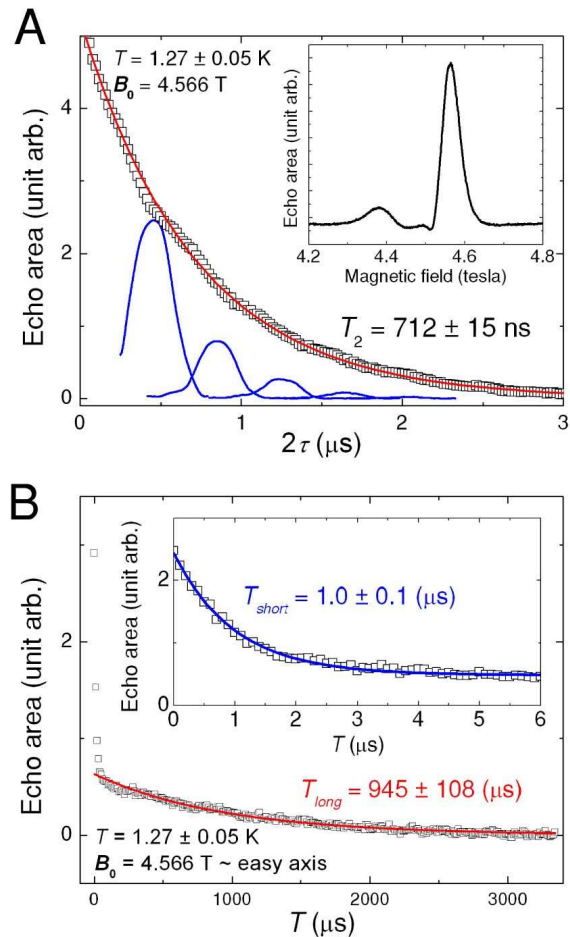

FIG. 2: (A) Echo signals and echo decay as a function of 2τ. The solid line is a fit using a single exponential. Inset shows echo-detected EPR signals as a function of magnetic field. (B) Echo decay measured by a stimulated echo sequence. Inset shows a measurement of the echo decay in a short timescale. Long decay curve was fit by a single exponential $e^{-T/T_{long}}$ as shown in red solid lines while short decay curve was fit by a double exponential $Ae^{-T/T_{long}} + Be^{-T/T_{short}}$ with $T_{long} = 945$ μs.

rate by,

$$\frac{1}{T_2} = A \sum_{m_S=-10}^{9} W(m_S) P_{m_S} P_{m_S+1} + \Gamma_{res} \qquad (2)$$

$$P_{m_S} = \frac{e^{-\beta E(m_S)}}{Z} \qquad (3)$$

where A is a temperature independent parameter, $\beta = 1/(k_B T)$, Z is the partition function of the Fe_8 SMM spin system and Γ_{res} is a residual relaxation rate which comes from other temperature independent decoherence sources. The flip-flop transition probability with two
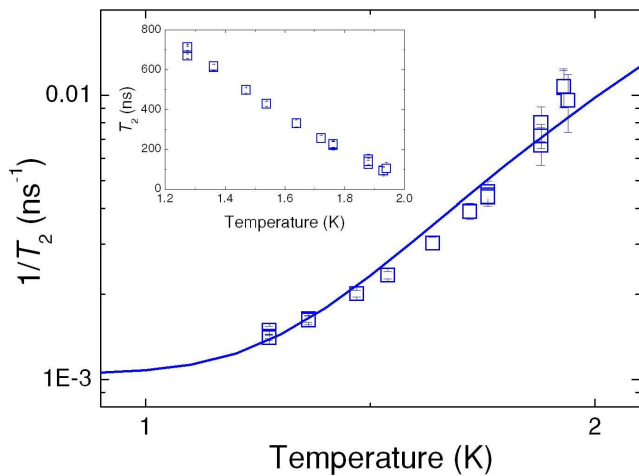
FIG. 3: Temperature dependence of $1/T_2$. Data with error bars are shown by square dots and a simulation of spin bath decoherence is shown by a solid line. The inset shows a plot of T_2 vs. temperature.

electron spins $W(m_S)$ is given by,

$$W(m_S) = | < m_S + 1, m_S | S_1^+ S_2^- | m_S, m_S + 1 > |^2$$
$$+ | < m_S, m_S + 1 | S_1^- S_2^+ | m_S + 1, m_S > |^2. \quad (4)$$

Using the Eq. (1)-(4), we plotted the temperature dependence of T2 as shown in Fig. 3. The proposed model is in good agreement with the experimental data. Therefore the result strongly supports the decoherence mechanism caused by the Fe$_8$ spin bath fluctuation. The best agreement is obtained with $\Gamma_{res} = 1.0 \times 10^{-3}$ ns^{-1}, which corresponds to $T_2 = 1$ μs. This residual decoherence is likely related to hyperfine couplings to $I = 1/2$ for ^{57}Fe (2.1 % natural abundance) and $I = 1/2$ for proton nuclear moments in the molecules [27], and represents the decoherence time one would expect in a highly diluted single crystal of Fe$_8$ SMM. SMM crystals grown with replaced by deuterium ($I = 1$) and with isotopically pure ^{56}Fe ($I = 0$) may have even longer low-temperature decoherence times. The given values of the Γ_{res} and A in Eq. (2) also lead to a few ns of the minimum T_2 around 10 K. Therefore this indicates that the increase of T_2 by polarizing the spin bath is more than two orders of magnitude.

In summary, the temperature dependence of the spin decoherence time T_2 of Fe$_8$ SMMs was measured between 1.27 K and 1.93 K. With increasing temperature, T_2 decreases by an order of magnitude from 714 ns at 1.27 K. The identification of the main and the second decoherence sources for the Fe$_8$ SMM and the demonstration of the suppression of Fe$_8$ spin decoherence is particularly important to engineer molecular magnets for future quantum information processing applications. These measurements also establish that high-frequency pulsed EPR at low temperatures provides access to a frontier of spin decoherence in electron spin systems.

[1] D. Gatteschi, R. Sessoli, and J. Villain, in *Molecular nanomagnets* (Oxford Univeristy Press, New York, 2006).
[2] J. R. Friedman, M. P. Sarachik, J. Tejada, and R. Ziolo, Phys. Rev. Lett. **76**, 3830 (1996).
[3] L. Thomas et al., Nature **284**, 145 (1996).
[4] C. Sangregorio, T. Ohm, C. Paulsen, R. Sessoli, and D. Gatteschi, Phys. Rev. Lett. **78**, 4645 (1997).
[5] W. Wernsdorfer and R. Sessoli, Science **284**, 133 (1999).
[6] C. M. Ramsey et al., Nature Phys. **4**, 277 (2008).
[7] A. Caneschi et al., J. Am. Chem. Soc. **113**, 5873 (1991).
[8] A.-L. Barra et al., Europhys. Lett. **35**, 133 (1996).
[9] S. Hill, R. S. Edwards, N. Aliaga-Alcalde, and G. Christou, Science **302**, 1015 (2003).
[10] A. Mukhin, B. Gorshunov, M. Dressel, C. Sangregorio, and D. Gatteschi, Phys. Rev. B **63**, 214411 (2001).
[11] M. N. Leuenberger and D. Loss, Nature **410**, 789 (2001).
[12] L. Bogani and W. Wernsdorfer, Nature mater. **7**, 179 (2008).
[13] G. de Loubens et al., J. Appl. Phys. **103**, 07B910 (2008).
[14] E. del Barco, A. D. Kent, E. C. Yang, and D. N. Hendrickson, Phys. Rev. Lett. **93**, 157202 (2004).
[15] A. Ardavan et al., Phys. Rev. Lett. **98**, 057201 (2007).
[16] C. Schlegel, J. vanSlageren, M. Manoli, E. K. Brechin, and M. Dressel, Phys. Rev. Lett. **101**, 147203 (2008).
[17] S. Takahashi, R. Hanson, J. van Tol, M. S. Sherwin, and D. D. Awschalom, Phys. Rev. Lett. **101**, 047601 (2008).
[18] K. Wieghardt, K. Pohl, I. Jibril, and G. Huttner, G. Angew. Chem., Int. Ed. Engl. **23**, 77 (1984).
[19] G. W. Morley, L.-C. Brunel, and J. van Tol, Rev. Sci. Instrum. **79**, 064703 (2008).
[20] J. van Tol, L.-C. Brunel, and R. J. Wylde, Rev. Sci. Instrum. **76**, 074101 (2005).
[21] D. Zipse, J. M. North, N. S. Dalal, S. Hill, and R. S. Edwards, Phys. Rev. B **68**, 184408 (2003).
[22] A. Schweiger and G. Jeschke, in *Principles of Pulse Electron Paramagnetic Resonance* (Oxford Univeristy Press, New York, 2001).
[23] S. Bahr, K. Petukhov, V. Mosser, and W. Wernsdorfer, Phys. Rev. Lett. **99**, 147205 (2007).
[24] M. Bal et al., Europhys. Lett. **82**, 17005 (2008).
[25] A. Morello, P. C. E. Stamp, and I. S. Tupitsyn, Phys. Rev. Lett. **97**, 207206 (2006).
[26] C. Kutter et al., Phys. Rev. Lett. **74**, 2925 (1995).
[27] W. Wernsdorfer et al., Phys. Rev. Lett. **84**, 2965 (2000).